

Article

Marine Snow Aggregates are Enriched in Polycyclic Aromatic Hydrocarbons (PAHs) in Oil Contaminated Waters: Insights from a Mesocosm Study

Hernando P. Bacosa ^{1,2,3,*} , Manoj Kamalanathan ¹ , Joshua Cullen ¹ , Dawei Shi ⁴, Chen Xu ², Kathleen A. Schwehr ², David Hala ¹, Terry L. Wade ^{4,5}, Anthony H. Knap ^{4,5}, Peter H. Santschi ^{2,5} and Antonietta Quigg ^{1,5} 

- ¹ Department of Marine Biology, Texas A&M University at Galveston, Galveston, TX 77553, USA; manojka@tamug.edu (M.K.); joshcullen@ufl.edu (J.C.); halad@tamug.edu (D.H.); quigga@tamug.edu (A.Q.)
- ² Department of Marine and Coastal Environmental Science, Texas A&M University at Galveston, Galveston, TX 77553, USA; xuc@tamug.edu (C.X.); schwehrk@tamug.edu (K.A.S.); santschi@tamug.edu (P.H.S.)
- ³ Department of Biological Sciences, College of Science and Mathematics, Mindanao State University-Iligan Institute of Technology, Iligan, Lanao del Norte 9200, Philippines
- ⁴ Geochemical and Environmental Research Group, Texas A&M University, College Station, TX 77845, USA; dvshi@tamug.edu (D.S.); t-wade@geos.tamu.edu (T.L.W.); tknap@geos.tamu.edu (A.H.K.)
- ⁵ Department of Oceanography, Texas A&M University, College Station, TX 77843, USA
- * Correspondence: herbacs3001@gmail.com

Received: 11 August 2020; Accepted: 2 October 2020; Published: 7 October 2020



Abstract: Marine snow was implicated in the transport of oil to the seafloor during the Deepwater Horizon oil spill, but the exact processes remain controversial. In this study, we investigated the concentrations and distributions of the 16 USEPA priority polycyclic aromatic hydrocarbons (PAHs) in marine snow aggregates collected during a mesocosm experiment. Seawater only, oil in a water accommodated fraction (WAF), and Corexit-enhanced WAF (DCEWAF) were incubated for 16 d. Both WAF and DCEWAF aggregates were enriched in heavy molecular weight PAHs but depleted in naphthalene. DCEWAF aggregates had 2.6 times more total 16 PAHs than the WAF (20.5 vs. 7.8 µg/g). Aggregates in the WAF and DCEWAF incorporated 4.4% and 19.3%, respectively of the total PAHs in the mesocosm tanks. Our results revealed that marine snow sorbed and scavenged heavy molecular weight PAHs in the water column and the application of Corexit enhanced the incorporation of PAHs into the sinking aggregates.

Keywords: polycyclic aromatic hydrocarbons (PAHs); marine snow; oil spill; mesocosm; Gulf of Mexico; water accommodated fraction (WAF)

1. Introduction

The 2010 Deepwater Horizon (DwH) blowout was one of the worst environmental disasters in US history that released about 4.4 million barrels of crude oil into the Gulf of Mexico [1]. The oil was released for 87 days from the Macondo wellhead, located 80 km off the Louisiana coast and at the seafloor 1500 m below the sea surface. A vast area of the northern Gulf of Mexico was covered with oil slicks and oil sheen for weeks after the release [2]. In an attempt to mitigate the impacts of the oil spill, ~7 million liters of Corexit dispersants were applied to the surface and injected at the wellhead [3]. The spill also resulted in a subsurface continuous plume of oil up to 35 km in length [4].

The Macondo crude oil is a type of light Louisiana sweet crude oil with 16% aromatic hydrocarbons and 74% saturated hydrocarbons, and 10% polar hydrocarbons [5]. Although polycyclic aromatic

hydrocarbons (PAHs) comprise a small percentage of the oil, these contaminant compounds are of primary concern [6–8]. The US Environmental Protection Agency (EPA) has classified 16 PAHs as priority pollutants because of their toxicity, carcinogenicity, and prevalence and persistence in the environment [9]. PAHs have been the focus of several studies in fish, seafood, coastal water and sediment, and the deep-sea following the DwH spill [10–16].

It was estimated that roughly 50% of the spilled Macondo crude oil was burned, recovered, naturally dispersed, evaporated, dissolved, or chemically dispersed, while the rest could not be accounted for [3]. Materials associated with the DwH spill, which largely consist of oil-related compounds, bacterial biomass, and organic detritus, were found in the seafloor sediment in areas up to 8 km from the wellhead [17,18]. These materials are believed to be transported into the seabed by sinking marine snow [19]. Marine snow is a natural process that is characterized by a shower of particle aggregates formed by processes that occur in the world's oceans, consisting of macroscopic aggregates of exopolymeric substances (EPS), detritus, living organisms, and inorganic matter [20,21]. Several studies showed that marine snow formation occurred in the Gulf of Mexico during the release and played an important role in the fate and transport of oil to the deep sea through the formation of marine oil snow (MOS) [16,19,22]. The rapid sedimentation of MOS was suggested to transport the hydrocarbons to the seafloor resulting in the deposition of 4–31% of the DwH oil to the seafloor [15,23–29]. This broad estimate has sparked widespread interest and has been a subject of debate in the scientific community and beyond. Moreover, the northern Gulf of Mexico is also characterized by high temperature and intense solar radiation that strongly affect the biodegradation and photooxidation of oil and the formation of marine snow [30–33].

Marine snow aggregates are composed of various particles embedded in a matrix of sticky mucus of high molecular weight exudates, i.e., EPS secreted by bacteria and phytoplankton [34–37]. The production and character of the EPS is affected by the concentration of oil and chemical dispersant [35,38]. Conversely, the composition of EPS produced could also affect the fate of oil and dispersant. Particularly, the dispersion of oil and incorporation of the hydrocarbons into aggregates depends on the amphiphilic properties of the EPS [28,34,37,39]. Laboratory studies using roller-table systems were performed to investigate the formation of sinking marine snow using oil in water concentrations ranging from 600 to 10,000 $\mu\text{g/L}$ [19,40–44]. These experiments showed that sinking mucus webs, flocs, and oil aggregates were formed within 1 to 7 d of incubation. The presence of Corexit dispersant resulted in a lower number of aggregates, but appeared to increase the sinking rates and the incorporation of oil into aggregates [43,45]. In addition, Corexit not only enhanced dissolution of alkanes but also enhanced the incorporation of low-molecular-weight *n*-alkanes ($\text{C}_9\text{--C}_{18}$) into MOS [42]. Moreover, roller-table experiments facilitated a consistent mixing of the oil in a closed-system and was characterized by a centripetal motion and constant contact of the oil in water to the forming aggregates. Hence, the incorporation of oil particles into the sinking mucus was forced or inevitable. On the other hand, the ocean is an open-system such that the formed aggregates on the surface that are denser than seawater are vertically transported deeper into the water column. The contribution of the process of marine snow sedimentation to the removal of oil during the DwH were not established [21].

To fill these knowledge gaps, mesocosm experiments were conducted to mimic and inform our understanding of the formation of marine snow in natural seawater, in the presence of oil and oil plus dispersant [27,28,34,46–51]. The mesocosms were 110-L glass tanks (dimension in cm 75 h \times 40 w \times 40 w) filled with a water accommodated fraction of oil (WAF), and oil plus Corexit dispersant in a chemically enhanced water accommodated fraction (CEWAF), or the diluted CEWAF (DCEWAF), and natural seawater collected from the Gulf of Mexico (controls). WAF, referred to as a water-soluble fraction of oil, is a solution of the dissolved fractions of oil (mainly highly soluble low molecular weight hydrocarbon compounds) released when oil is mixed and stirred with water [34,35,46]. Using WAF in the mesocosms mimicked realistic oil concentrations of half to tens of mg/l found during the DwH oil spill [46,52]. After 3 days of incubation, the PAHs and *n*-alkanes were significantly removed in these

mesocosm tanks. Known hydrocarbon-degrading bacteria likely responsible for the degradation of oil dominated [48]. Marine snow aggregates also formed in the tanks and were characterized [27,37,39,51]. The sedimentation efficiency of petroleum-derived carbon in sinking marine snow ranged from 0.1% to 27% in WAF, CEWAF and DCEWAF tanks [27,37]. Corexit enhanced the incorporation of oil into the marine snow aggregates, and the oil that accumulated in these aggregates had undergone rapid weathering and depletion of alkanes [47]. Moreover, the oxygenation patterns revealed that the oil components associated with the aggregates were degraded [51]. In this study, we report the concentrations and distributions of the 16 parent PAHs in marine snow aggregates in the mesocosms. We found that the marine snow aggregates have elevated concentrations of high molecular weight PAHs and the addition of Corexit increased the incorporation of these compounds into the aggregates.

2. Materials and Methods

2.1. Mesocosm Experiments

A long-term mesocosm experiment was conducted from May to June 2017 in 110-L borosilicate glass tanks using surface water collected from the Gulf of Mexico adjacent to Galveston (TX, USA). The seawater was pre-filtered through charcoal to remove particles and used for the production of WAF (oil only) and CEWAF (oil + Coxit dispersant) using the 170-mL baffled recirculating tank (BRT) system following established methods [46]. Briefly, the WAF was prepared by mixing a total of 24 mL of oil into 130 L of the seawater in the BRT stirred for 14 h. The Macondo Surrogate Oil (specific gravity 0.86 g/mL) provided by BP was used in this study. The Macondo Surrogate Oil was from the Marlin Platform Dorado (SO-20120211-MPDF-003) and is similar to the DWH Oil [46]. The CEWAF was prepared by premixing Corexit (specific gravity 0.949 g/mL) with Macondo Surrogate Oil at a ratio of 1:20 (*v/v*). Diluted CEWAF, referred to here as DCEWAF, was prepared by diluting CEWAF with seawater at a ratio of 1:9. About 80 L of WAF, DCEWAF, and seawater (control) was then transferred to each mesocosm tank. Prior to the initiation of the experiment, a plankton concentrate collected from the marina of Texas A&M University at Galveston was added to each tank. Six replicate tanks were prepared each for control, WAF, and DCEWAF treatments. The experiment was conducted for 16 days at 20 °C with 12 h light:dark cycles using gowlux fluorescent lights providing 50–100 $\mu\text{mole-quanta}/\text{m}^2/\text{s}$.

MOS aggregates formed in the tanks within 24 h. After 3 d, water samples were collected from three replicate tanks from each treatment for the analysis of hydrocarbons. After decanting the majority of the water body, the aggregates that sank at the bottom of the three replicate tanks were collected at 4 d and transferred to pre-combusted glass jars. The remaining three tanks from each treatment were sampled with water for hydrocarbon analysis at 15 d. Similarly, marine snow aggregates that sank at the bottom of each tank were collected at 16 d. The aggregate samples were placed on pre-combusted GF/F filter and resuspended in nanopure water. The samples were stored in $-20\text{ }^{\circ}\text{C}$, and subsequently freeze-dried prior to analysis (78060 FreeZone Bulk Tray Dryer, Labconco).

2.2. PAH Extraction and Analysis from the Aggregates

The freeze-dried sample was weighed and transferred to 7-mL polypropylene tubes containing ceramic beads to increase homogenization (Fisher Scientific, Waltham, MA, USA). A mixture of deuterated standards naphthalene- d_8 , phenanthrene- d_{10} , and perylene- d_{12} , was added using a microsyringe, prior to extraction [35,53]. The PAHs were extracted following established protocols [54]. Briefly, 3 mL of 1:1 *v/v* hexane:ethyl acetate was added to the tube, then placed in a Fisherbrand™ Bead Mill 4 Homogenizer (Fisher Scientific, Waltham, MA, USA) and homogenized at a processing power of 150 g for 2 min. The homogenate was transferred to an acid-washed 50-mL glass tube, and 2 mL of hexane/ethyl acetate was added and placed in a Branson Ultrasonics™ M2800 Ultrasonic Bath (Fisher Scientific, Waltham, MA, USA) for 30 min to extract PAHs into the solvent. The sample was centrifuged at $2000\times g$ for 5 min to separate the homogenates from the solvent phase. The supernatant was pipetted to 20-mL glass vials. This extraction process was performed thrice. The extract was

then evaporated under N₂ to ~1 mL and exchanged with hexanes. The sample was then cleaned-up using a chromatographic column dry-packed with 3 g of activated silica gel and topped with 1 cm of anhydrous sodium sulfate following established procedures [30,32,53,55]. Finally, the extract was concentrated to 200 µL prior to analysis.

An aliquot of the extract (100 µL) was transferred to a glass insert in a 2-mL chromatographic amber vial. The following PAHs were analyzed: Naphthalene (Nap), Acenaphthylene (Acy), Acenaphthene (Ace), Fluorene (Flu), Phenanthrene (Phe), Anthracene (Ant), Fluoranthene (Flt), Pyrene (Pyr), Benzo[a]anthracene (BaA), Chrysene (Chr), Benz[b]fluoranthene (BbF), Benz[k]fluoranthene (BkF), Benzo[a]pyrene (BaP), Indeno [1,2,3-cd]pyrene (Ind), Dibenzo[a,h]anthracene (Dba), and Benz[g,h,i]perylene (BghiP). The PAHs were analyzed on a Hewlett Packard HP-6890 gas chromatograph coupled to Agilent 5973 inert mass selective detector (GC-MS). Sample (2 µL) was injected into the system in splitless mode and operated in the selective ion monitoring (SIM) mode. The PAHs were resolved using a 30-m long Agilent DB-5MS column. The operating conditions are specified elsewhere [53,54]. Quantification of the PAHs was determined by the response factors determined from a 10-point calibration curve. The reported concentrations of target analytes are recovery corrected. The concentrations are expressed as concentrations in aggregate dry weight. The recovery rates for naphthalene-d₈, phenanthrene-d₁₀, and perylene-d₁₂, were 88.6 ± 7.5%, 93.6 ± 8.7%, and 95.3 ± 5.9%.

2.3. PAH Extraction and Analysis from Water Samples

Water samples (3.5 L) were collected from each mesocosm tank at day 0, 3, and 15 and preserved with 100 mL of dichloromethane (DCM) until analysis. Deuterated PAHs standards (100 µL) was added to each sample prior to extraction to determine the recovery efficiency. The samples were then extracted twice with DCM, concentrated and purified with alumina/silica gel chromatographic columns, and eluted by DCM/pentane mixture (1/1 v/v). The extract was concentrated to a final volume of 1 mL and analyzed by Hewlett-Packard 6890 gas chromatograph (GC) coupled with a Hewlett-Packard 5973 mass selective detector [46]. The PAHs were separated in a DB-5 MS fused silica capillary column (30 m × 0.25 mm i.d., 0.25 µm film thickness (J&W Scientific, Fossen, CA, USA). The initial oven temperature was 60 °C, ramped at 15 °C/min to 150 °C, 5 °C/min to 220 °C, and finally at 10 °C/min to a final temperature of 300 °C with a final holding time of 10 min. The PAHs were identified based on comparison with the calibration standards and qualified based on the response of the parent PAHs.

The sedimentation efficiency of the PAHs at 16 d was calculated according to the formula:

$$\frac{\text{PAH in MOS aggregates at 16 d}}{\text{PAH in water at 0 d}} \times 100\%$$

2.4. Statistical Analysis

All results are presented as means plus or minus the standard deviation. The significant differences in the means of total PAHs in the aggregates was determined using a one-way analysis of variance (ANOVA) in the PAST software package, V2.17 [56]. The differences among the means were further tested by Tukey's HSD test.

3. Results

All the 16 USEPA priority pollutant PAHs were present in almost all aggregate samples. The mean concentration of total PAHs in aggregates in Control tanks were 1.72 µg/g and 2.64 µg/g at 4 d and 16 d, respectively (Figure 1). The WAF aggregates were higher than the control and contained 7.42 µg/g (4 d) and 8.12 µg/g (16 d) of PAHs. The highest concentrations of PAHs were observed in DCEWAF tanks, where they were 21.27 µg/g (4 d) and 19.79 µg/g (16 d). It is noteworthy that the PAHs in the WAF aggregates were 3–4 times more abundant than the control, while the DCEWAF aggregates were

approximately 2.6-fold greater than those in the WAF. Interestingly, there was no significant difference in the total PAHs concentrations between 4 d and 16 d in Control, WAF, and CEWAF aggregates ($p > 0.05$).

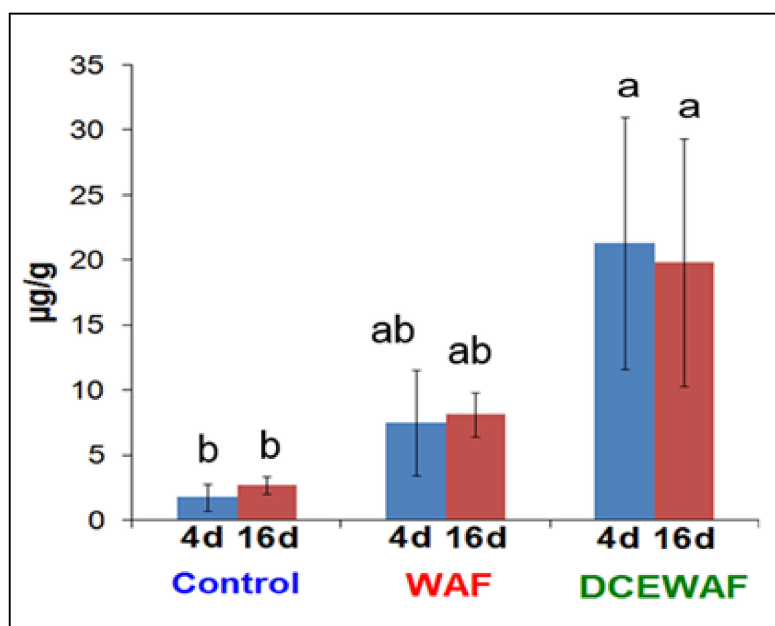


Figure 1. Total PAHs concentrations in marine snow aggregates in Control, WAF, and DCEWAF mesocosm tanks at 4 d and 16 d. Error bars represent standard deviations among replicates. Different letters are significantly different ($p < 0.05$) according to Tukey's HSD mean separation test.

Individual PAHs compounds occurred in variable concentrations. Both WAF and DCEWAF aggregates were depleted in naphthalene but enriched in phenanthrene and 4-ring PAHs (Figure 2). Phenanthrene, fluoranthene, pyrene, and chrysene represented roughly 68% and 77% of total PAHs in WAF and DCEWAF aggregates, compared to ~10% (WAF) and 20% (DCEWAF) in the starting seawater. On the other hand, naphthalene, which comprised 74–88% of the total PAHs in seawater at the beginning, only represented 1.40% and 0.70% in WAF and DCEWAF aggregates, respectively. The four to six-ring PAHs are commonly classified as heavy molecular weight (HMW) PAHs. Taken together, the aggregates were predominantly composed of HMW PAHs, represented 75% in WAF and 71% in DCEWAF (Figure 3). HMW PAHs were only 1.1% (WAF) and 4.0% (DCEWAF) of the total PAHs at the start of the experiment. Phenanthrene, fluoranthene, pyrene, and chrysene in 4 d and 16 d DCEWAF aggregates were 2.5–3-fold greater than the corresponding WAF aggregates. Moreover, DCEWAF had elevated concentrations of 5–6 ring PAHs at varying levels (Figure 2). It is worth mentioning that there were no appreciable differences in the concentrations between 4 d and 16 d across all compounds.

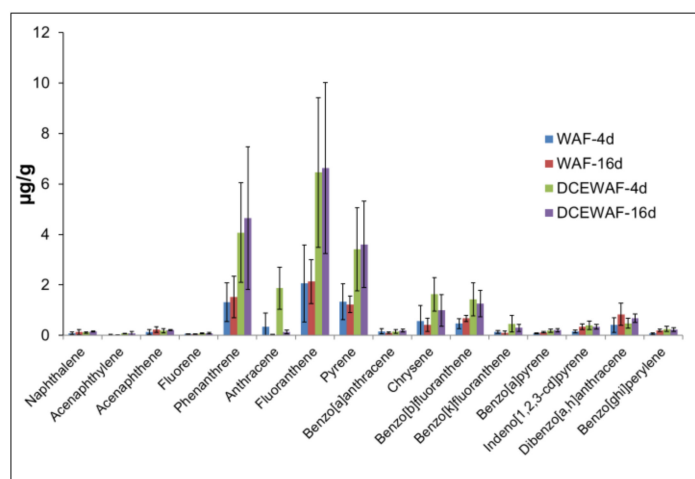


Figure 2. Concentrations of individual PAHs in the marine snow aggregates in WAF and DCEWAF mesocosm tanks at 4 d and 16 d. Error bars represent standard deviations among replicates.

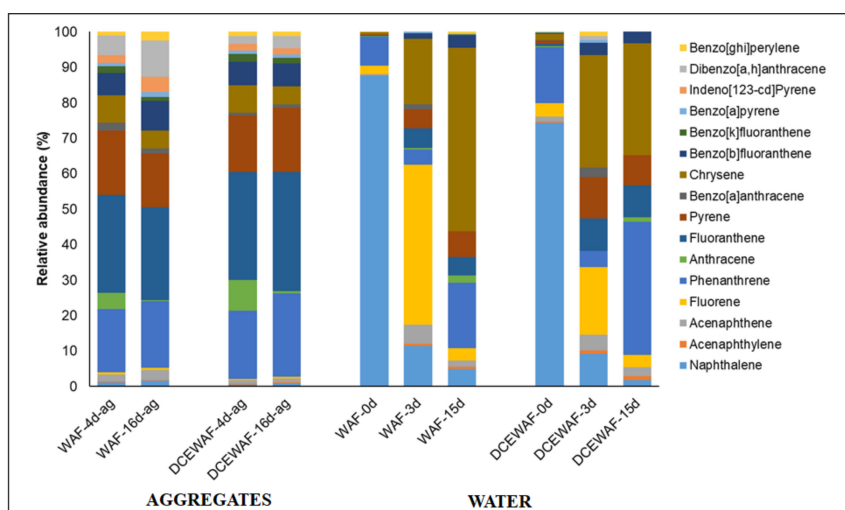


Figure 3. Relative abundances of PAHs in the marine snow aggregates and the water column.

The concentration of total PAHs in WAF and DCEWAF water decreased by 97.6% (18.94 µg/L to 0.45 µg/L) and 97.1% (7.37 µg/L to 0.21 µg/L), respectively, within 3 days (Table 1). At 15 d, the concentrations were further reduced by 99.8% in WAF and 98.9% in DCEWAF. The initial concentration of total PAHs in WAF was 2.5 times greater than in the DCEWAF tank, mainly due to naphthalene, which accounted for 88% of the total PAHs in the WAF, but only 74% in the DCEWAF (Figure 3). Naphthalene stood out as the most dominant PAH due to its high aqueous solubility (31 mg/L at 25 °C). Excluding naphthalene, the total of 15 PAHs at the start of the experiment was 2.34 µg/L for WAF and 1.90 µg/L for DCEWAF.

Table 1. The concentration of total of 16 PAHs in the water column.

Treatment/Day	0 d	3 d	15 d
Control	0.085 ± 0.025	0.081 ± 0.014	0.044 ± 0.005
WAF	18.94 ± 11.28	0.45 ± 0.53	0.042 ± 0.011
DCEWAF	7.37 ± 8.98	0.21 ± 0.03	0.081 ± 0.035

We also were able to calculate the sedimentation efficiency, which is the percentage of the amount of the PAHs incorporated into the aggregates to the initial PAHs (in aqueous phase) in the mesocosm tank [27,37]. We only computed this for samples taken at 16 d because of greater confidence in the sampling efficiency and the volume of water collected from the mesocosm tanks. The average sedimentation efficiency of the PAHs, excluding naphthalene, in the WAF aggregates, was 32.5% while that in DCEWAF tanks was 48.9%, or 1.5 times higher than in the WAF (Figure 4). This result indicates that the presence of Corexit dispersant enhanced the incorporation of the PAHs, particularly those greater 2 rings, into the aggregates from the water column. Sedimentation efficiency increased with an increasing number of rings. The 2-ring naphthalene (WAF—0.13%; DCEWAF—0.36%) and 3-ring fluorene (WAF—1.19%; DCEWAF—1.64%) were poorly incorporated. The faster disappearance of naphthalene from the system due to its volatility might be a factor in its low incorporation. Sedimentation efficiency increased for phenanthrene for both WAF (8.78%) and DCEWAF (17.80%), and increased further for pyrene, which was 162% and 199% for WAF and DCEWAF, respectively. Surprisingly, the values of sedimentation efficiency had exceeded 100% for most 4–5 ring PAHs except for chrysene, which was roughly 45%. It appears that an efficiency of >100% was mainly caused by an inaccuracy in a constant factor (e.g., the total amount of aggregates had to be estimated from smaller assays). Nonetheless, the relative trends in the sedimentation efficiency would still be valid.

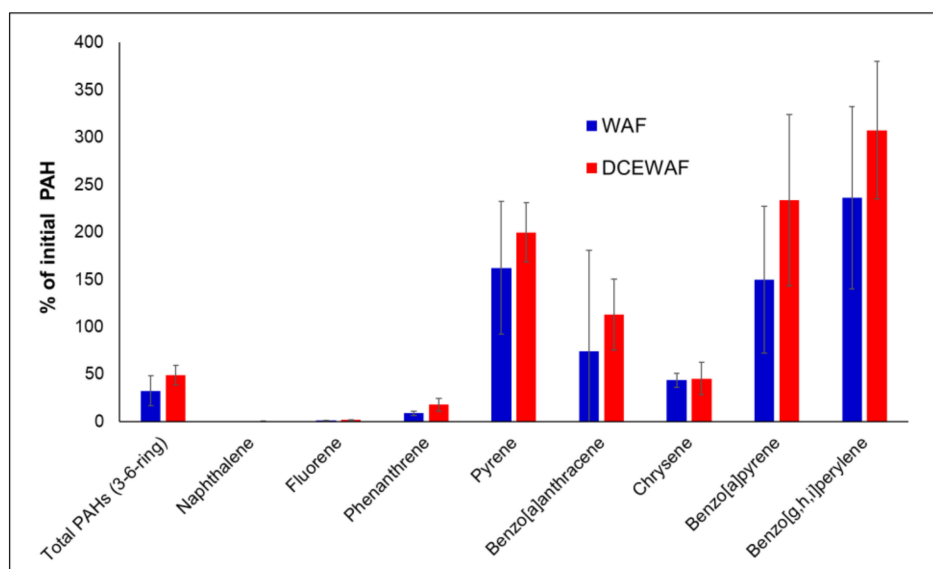


Figure 4. PAHs sedimentation efficiency in the 16 d marine snow aggregates relative to the initial PAH concentrations in the aqueous phase. Error bars represent standard deviations among replicates.

4. Discussion

The 16 PAHs analyzed in this study represented ~1% of the total petroleum hydrocarbons (TPHs) in the oiled treatments, but this group of compounds pose a greater risk to the environment due to their toxic, carcinogenic, and mutagenic properties [6]. Many PAHs are also resistant to biodegradation, are recalcitrant and persist in the environment [57–61]. This study attempted to determine the distribution and concentrations of parent PAHs in marine snow aggregates, which eventually become part of surface sediment matrix in marine environments. The disappearance of the PAHs in the water column did not mean that they were degraded, however, but rather that they were scavenged by marine snow and incorporated into the sinking aggregates that settled at the bottom of the mesocosm tanks. Particularly, heavy molecular PAHs were greatly enriched in the aggregates, but not naphthalene. Naphthalene amounted to roughly 80% of the initial PAHs in the mesocosm tanks. Two-ring PAHs, including naphthalene (aqueous solubility at 25 °C = 31 mg/L) and its alkylated homologues are volatile and dissolve in water, making them more available for biological uptake and evaporation [62–65].

Loh et al. [66] reported that the loss of PAHs through evaporation could account for more than 10% within 24 h, mainly due to the disappearance of naphthalene and its alkylated homologues. The loss due to evaporation, which is beyond the scope of this study, could be one important mechanism of the disappearance of the naphthalene from the mesocosm and its lower concentration in the MOS aggregates. Naphthalene and many 3-ring PAHs such as fluorene, acenaphthene, and acenaphthylene also have relatively lower adsorbability [67]. The mesocosm tanks are open system and bacterial density increased in the oiled tanks with a greater abundance of known-hydrocarbon degraders [48]. The combination of these factors was likely responsible for the rapid disappearance of naphthalene in the water column and poor incorporation into the marine snow.

The marine snow aggregates are complex matrices composed of sediment and mineral particles, EPS, and cellular materials. PAHs are considered as particle-reactive pollutants [68]. In particular, heavy molecular weight PAHs have low volatility and are hydrophobic that are predominantly in solid-state with high affinity for adsorption to sediment and organic particles, and absorbed or bioconcentrated by organisms [6,69]. They quickly adsorb to the organic phase of suspended particles and are deposited with them into the sediment [60,70]. The adsorption of PAHs in marine snow aggregates generally increased with an increasing number of rings, which is consistent with their values of the octanol-water partition coefficient (K_{ow}) and organic carbon sorption partition coefficient (K_{oc}) [71]. K_{ow} is a useful physical property to model the fate and transport of organic pollutants in aquatic and terrestrial systems [6]. HMW PAHs have higher K_{ow} values and have a greater tendency to be adsorbed to sediment and suspended particles. Furthermore, HMWs are also recalcitrant and resistant to biodegradation, even in the presence of putative degrading bacteria [59–65]. A wide array of microorganisms, including fungi, algae, and bacteria, are known to degrade low molecular PAHs but few HMW PAHs [57–62]. In this mesocosm experiment, marine snow was acting as an organic-rich particle that sorbed and scavenged the PAHs in the water column and subsequently sank to the bottom. The mesocosm tanks have innate inhomogeneity of mechanically-dispersed oil-water mixture (WAF) and chemically-dispersed oil–water mixture (CEWAF) [46]. The sedimentation of the PAHs by MOS can be achieved by sedimentation through absorption of oil droplets (true-sedimentation), and sedimentation by scavenging dissolved PAHs. Our mesocosm experiment was not designed to differentiate these two types of sedimentation of PAHs and what we report here is a combination of these two mechanisms. The presence of suspended particulate matter (SPM) increased significantly oil stability for both mechanically-dispersed oil (WAF) and chemically-dispersed oil (DCEWAF and CEWAF), yet the latter usually has a higher oil dispersion effectiveness [72]. The stability of MOS-like aggregates, such as the mechanically and chemically-dispersed oil with SPM, depends on the physicochemical properties of the mineral particle [72]. The MOS is a complex matrix of various substances and mineral particles, where its surface properties such as polarity, hydrophobicity, and expandable interlayer spaces can affect the affinity of MOS towards oil, which in turn affects the stability of MOS-oil/PAHs interactions [73,74]. In natural environments, aggregated MOS can resurface once the size of MOS increases and density decreases [75]. However, we did not observe the resurfacing of the sedimented MOS in the bottom of the mesocosm tanks, which could be attributed to the lack of breaking waves acting on the water in the tanks. Moreover, while we did not directly investigate the stability of the scavenging MOS aggregate, Passow et al. [76] reported a tighter packaging of this oil-EPS-mineral ternary system.

Corexit enhanced the incorporation of PAHs into the aggregates. The sedimentation efficiency that is equivalent to the amount of PAHs integrated into the aggregates relative to the initial amount in day 0 of the experiment in the water column showed that DCEWAF aggregates incorporated 4 times greater amounts than in the WAF tank. It should be noted that naphthalene alone comprised 74–88% of the initial PAHs in the oiled mesocosm. This means that roughly all HMWs compounds in the DCEWAF were carried by the sinking aggregates. In our previous mesocosm experiments, Corexit was also found to enhance the assimilation of petrocarbon into the micro- and macro-aggregates [37], but it was not known whether these petrocarbons are from alkanes, PAHs, or other oil components.

In this study, we revealed that the presence of Corexit increased the incorporation of PAHs, mainly the HMW compounds, into the marine snow aggregates. Dispersants, in general, facilitate the dispersion of oil through the formation of dispersant-coated oil droplets or partitioning of oil into micelles. Dispersants can also be sorbed into sediment and particle surfaces such as marine snow, forming larger hemimicelles/admicelles that in turn enhance the uptake of hydrophobic compounds such as PAHs which increases their dispersion in the water [77,78]. Corexit enhanced the apparent solubility of petroleum hydrocarbons and that the marine snow scavenged more of these dispersed hydrocarbons in DCEWAF, because of more hydrophobic sorption sites for PAHs [69]. Previous reports showed that the uptake of HMW pyrene was enhanced at low dispersant concentration, a concentration close to the Corexit in the DCEWAF [78]. Moreover, Corexit promotes the association between oil and proteins, assisting the emulsification of the oil in colloids and suspended particulate matter [28]. In roller tanks experiments, Corexit also increased the amount of oil trapped in marine oil snow and the concentration of alkanes [42,43]. In this mesocosm experiments, the removal of HMW PAHs in DCEWAF tanks was faster than that in WAF. This is likely not due to biodegradation because these compounds are recalcitrant, and not due to photooxidation because the lights used to illuminate the samples did not have any UV.

We have shown in this study that HMW PAHs were incorporated into particles faster in DCEWAF tanks and subsequently settled at the bottom of the tank with the aggregates. We carefully investigated, over time, the role of OSD (Corexit) in seven different mesocosm experiments on biological, chemical, and physical parameters through our experimental design, that included WAF, CWAF, DCWAF, and controls, all in triplicates, and varying experimental conditions [34]. Using natural radiocarbon analyses, Xu et al. [37] reported very similar sedimentation efficiencies that we obtained here. Chemically dispersed oil enhanced oil incorporation into the aggregates, but slowed down their settling due to added buoyancy to MOS of the incorporated oil. Dynamic biological and physicochemical changes of the oil components in the sinking aggregates, described by Hatcher et al. [47] and Wozniak et al. [51], indicated that components associated with the MOS showed a shift to more highly oxygenated components, which was particularly dramatic and rapid in the dispersant-containing treatments (DCEWAF and CEWAF) [51]. Such a change influenced the interactions between oil components, EPS, and mineral phases: in addition, the more polar (thus less hydrophobic) oil components possibly facilitated tighter packaging of this oil-EPS-mineral ternary system and led to a faster sinking velocity [76].

The PAHs in the aggregates seemed to have undergone negligible degradation between 4 d and 16 d. Typically, once sorbed in sediment, PAHs become more resistant to biotic or abiotic degradation [79]. Marine snow aggregates were reported to be hotspots of microbial activity being colonized by an abundant population of bacteria, with many known hydrocarbon degraders [48,80]. However, these bacteria might not be active in degrading PAHs, but utilizing alkanes and polysaccharides, the readily available carbon sources in the aggregates [39,81]. This is evident from our previous mesocosm experiments showing extracts from these aggregates showed characteristics of weathered oil depleted of *n*-alkanes and rich in oxygenated metabolites [47,51]. Linear alkanes are generally degraded preferably over PAHs by bacterial communities, and this phenomenon was also widely observed in the surface water of the Gulf of Mexico [30–32,82]. Oil degradation is a sequential process such that the *n*-alkanes are generally degraded first, followed by isoalkanes, and the recalcitrant HMW PAHs are among the least degraded and the slowest leaving a weathered oil containing numerous HMW PAHs at elevated concentrations [31,79]. It could also be possible that some PAHs were carried to the bottom with the weathered oil droplets. Moreover, incorporation of the recalcitrant HMW PAHs into the MOS, as facilitated by Corexit, likely resulted in a decrease in the MOS porosity, a subsequent tighter packaging, a higher excess density of the MOS, and eventually a faster sinking velocity [44,76], both of which were also related to higher protein to carbohydrate ratios [38,83]. This is a positive feedback to “protect” these PAHs components from biodegradation by the microbes in the

ambient water column. In addition, if Corexit was still associated with the aggregates, Corexit and its components could also be toxic to oil-degrading bacteria and could inhibit the PAH degraders [84,85].

In the Gulf of Mexico, the vertical flux of particle-bound PAHs plays a crucial role in the removal of these pollutants from the upper ocean to the deep-sea [67]. For the first time, Adhikari et al. [86] measured the sinking fluxes of particulate PAHs using tethered drifting sediment traps from 150 m to 350 m in the northern Gulf of Mexico, and found no changes in fluxes with depth. The PAHs in particulates were mainly of petroleum origin and were similar from one year to the next in 2012 and 2013. They concluded that PAHs are sorbed to the particles and are efficiently removed from the upper column via scavenging by settling marine particles [86]. In the current mesocom studies, we also observed that PAHs from the Control tanks were sorbed into the particles and settled at the bottom of the tanks. Although not directly comparable, the PAHs concentration in the control aggregates were comparatively higher than the sinking particles in the open ocean, but within the range of those in the coastal waters (Table 2).

Table 2. Comparison of PAHs concentration in sinking particles in this study and sediment trap particles from open ocean and coastal zones.

Study Area	∑PAHs (n)	Concentration (µg/g)	Reference
Control	16	0.754–2.81	This study
WAF	16	4.28–12.01	This study
DCEWAF	16	9.36–31.02	This study
Southwestern Black Sea (open ocean)	22	0.299–3.54	[87]
Mediterranean Sea (open ocean)	13	0.142–0.768	[88]
NW Arabia Sea (open ocean)	15	0.102–0.719	[89]
NW Mediterranean (coastal)	24	1.3–7.0	[90]
Baltic Sea (coastal)	18	0.55–4.25	[91]

The amount of oil deposited to the seafloor during the DwH spill is a subject of intense discussion, as the various estimates range from 4 to 31% of the total spilled volume [15,24–27]. A large fraction of these sedimenting fractions is attributed to the sinking marine oil snow by various authors [22,25,26]. If the spilled oil undergoes a significant change in chemical composition at a realistic concentration in the water column, as we had in the WAF or DCEWAF tanks, then the composition of the deposited material from the oil (weathered oil) is equally important. After all, the effects and toxicity of the oil residues on the environment and associated organisms largely depend on its composition, particularly of PAHs [92–96]. Adhikari et al. [70] reported that the impact of the DWH oil input into the deep-sea sediments was generally limited to the area close to the spill site. Based on the source diagnostic analysis of deep-sea surface sediment collected from various locations and distances from the DwH site, the PAHs composition was largely of heavy molecular weight. Romero et al. [15] reported on the PAHs composition of surface sediments collected from three sites selected based on the direction of the oil transport during the DwH, and another distal site as a control. These authors reported that the PAHs composition profiles were different for each site (Figure 5). It is not certain though which sample is largely affected by marine snow, but the profile of site DSH10, which was the closest to the DWH site, was different from the two other sites. Interestingly, the profiles of the PAHs obtained in the WAF and DCEWAF aggregates in this study closely resemble the profiles of the DSH10 samples collected in December 2010 and February 2011 (Figure 5). Whether PAH composition profiles can be used as a diagnostic tool for fingerprinting the contribution from marine oil snow, is a gargantuan task.

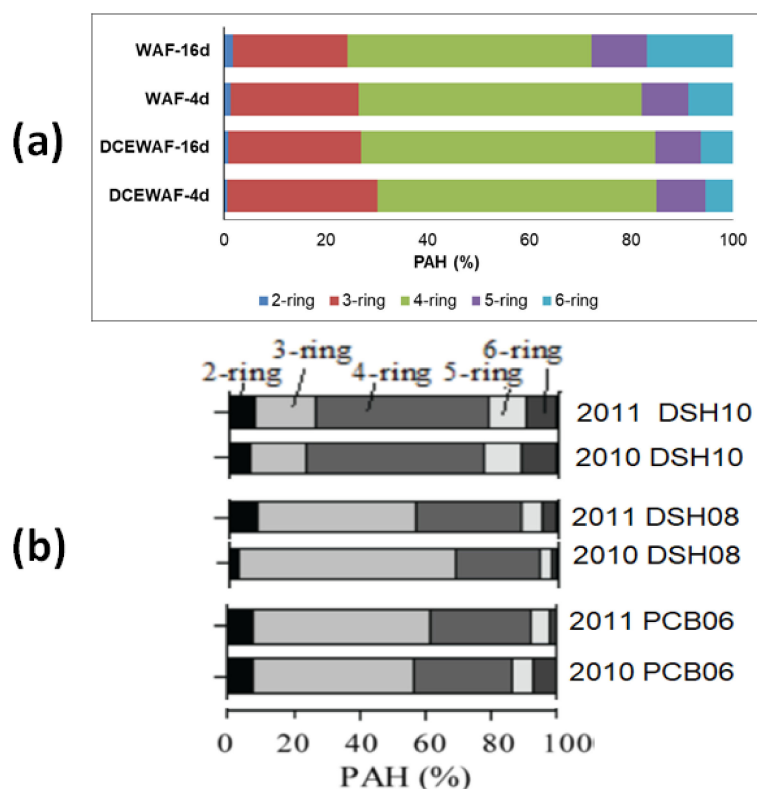


Figure 5. Comparison of the PAH composition profiles (2-, 3-, 4-, 5-, 6-ring) of the (a) WAF and DCEWAF aggregates in this study, (b) and the surficial sediment (0–2 mm) collected in the northern GoM after the DWH spill by Romero et al., (2015). Site DSH10 was the closest to the DWH location and PCB06 was the farthest.

5. Conclusions

This mesocosm study provides a unique opportunity to gain new insights into the fate of the toxic and carcinogenic PAHs in the marine environment, particularly in relation to the Deepwater Horizon oil spill. Overall, this mesocosm study revealed that the PAHs, particularly heavy-molecular weight compounds, were efficiently incorporated in marine snow and settled to the bottom of the tanks. The addition of Corexit dispersant resulted in a more extensive intake of PAHs by the aggregates. Once sorbed into these aggregates, the PAHs underwent negligible degradation. Taken together, our results suggest that the material deposited to the seafloor due to marine oil snow is highly weathered, depleted in aliphatic hydrocarbons, but enriched in heavy molecular weight PAHs, making it potentially more toxic to the deep-sea environments. Moreover, the application of Corexit enhanced the toxicity of the deposited material tremendously. These results improve our understanding of the role of marine snow on the fate of the PAHs in the deep-sea and deposition of these priority pollutants to the seafloor during and after oil spills.

Author Contributions: H.P.B.—carried out the experiment and analysis, prepared the manuscript; M.K., C.X., and K.A.S.—contributed to sample preparation and interpretation of the results; J.C. and D.H.—developed the analytical method; D.S.—analyzed PAHs in water; T.L.W., A.H.K., P.H.S., and A.Q.—conceived the idea of the mesocosm experiment, supervised the project, and acquired funding. All authors have read and agreed to the published version of the manuscript.

Funding: This research was funded by the grant from The Gulf of Mexico Research Initiative (GoMRI) through the research Consortium on Aggregation and Degradation of Dispersants and Oil by Microbial Exopolymers (ADDOMEx-2). Data are publicly available through the Gulf of Mexico Research Initiative Information & Data Cooperative (GRIIDC) at <https://data.gulfresearchinitiative.org> under doi:10.7266/5P8B7NWV.

Conflicts of Interest: The authors declare no conflict of interest.

References

1. Crone, T.J.; Tolstoy, M. Magnitude of the 2010 Gulf of Mexico oil leak. *Science* **2010**, *330*, 634. [[CrossRef](#)] [[PubMed](#)]
2. Klemas, V. Tracking oil slicks and predicting their trajectories using remote sensors and models: case studies of the Sea Princess and Deepwater Horizon oil spills. *J. Coast. Res.* **2010**, *26*, 789–797.
3. The Federal Intergovernmental Solutions Group (TFISG); Oil Budget Calculator Science and Engineering Team; National Oceanic and Atmospheric Administration (NOAA); U.S. Geological Survey (USGS); National Institute of Standards and Technology (NIST). *Oil Budget Calculator Deepwater Horizon*; Technical Documentation and Report to the National Incident Command; The Federal Intergovernmental Solutions Group (TFISG); Oil Budget Calculator Science and Engineering Team: Washington, DC, USA, 2010. Available online: http://www.restorethegulf.gov/sites/default/files/documents/pdf/OilBudgetCalc_Full_HQ-Print_111110.pdf (accessed on 21 October 2019).
4. Camilli, R.; Reddy, C.M.; Yoerger, D.R.; VanMooy, B.A.S.; Jakuba, M.V.; Kinsey, J.C. Tracking hydrocarbon plume transport and biodegradation at Deepwater Horizon. *Science* **2010**, *330*, 201–204. [[CrossRef](#)] [[PubMed](#)]
5. Reddy, C.M.; Arey, J.S.; Seewald, J.S.; Sylva, S.P.; Lemkau, K.L.; Nelson, R.K.; Carmichael, C.A.; McIntyre, C.; Fenwick, J.; Ventura, G.T.; et al. Composition and fate of gas and oil released to the water column during the Deepwater Horizon oil spill. *Proc. Natl. Acad. Sci. USA* **2012**, *109*, 20229–20234. [[CrossRef](#)] [[PubMed](#)]
6. Neff, J.M.; Stout, S.A.; Gunster, D.G. Ecological risk assessment of polycyclic aromatic hydrocarbons in sediments: Identifying sources and ecological hazard. *Integr. Environ. Assess. Manag.* **2005**, *1*, 22–33. [[CrossRef](#)]
7. Dominguez, J.J.; Chien, M.-F.; Inoue, C. Enhanced degradation of polycyclic aromatic hydrocarbons (PAHs) in the rhizosphere of sudangrass (*Sorghum × drummondii*). *Chemosphere* **2019**, *234*, 789–795. [[CrossRef](#)]
8. Dominguez, J.J.; Chien, M.-F.; Inoue, C. Hydroponic approach to assess rhizodegradation by sudangrass (*Sorghum × drummondii*) reveals pH- and plant age-dependent variability in bacterial degradation of polycyclic aromatic hydrocarbons (PAHs). *J. Hazard. Mater.* **2019**, *387*, 121695. [[CrossRef](#)]
9. ATSDR. *Toxicology Profile for Polyaromatic Hydrocarbons*; ATSDR's Toxicological Profiles on CD-ROM; CRC Press: Boca Raton, FL, USA, 2005.
10. Xia, K.; Hagood, G.; Childers, C.; Atkins, J. Polycyclic aromatic hydrocarbons (PAHs) in Mississippi seafood from areas affected by the Deepwater Horizon oil spill. *Environ. Sci. Technol.* **2012**, *46*, 5310–5318. [[CrossRef](#)]
11. Turner, R.E.; Overton, E.B.; Meyer, B.M.; Miles, M.S.; Hooper-Bui, L. Changes in the concentration and relative abundance of alkanes and PAHs from the Deepwater Horizon oiling of coastal marshes. *Mar. Pollut. Bull.* **2014**, *86*, 291–297. [[CrossRef](#)]
12. Brooks, G.R.; Larson, R.A.; Schwing, P.T.; Romero, I.; Moore, C.; Reichart, G.-J.; Jilbert, T.; Chanton, J.P.; Hastings, D.W.; Overholt, W.A.; et al. Sedimentation pulse in the NE Gulf of Mexico following the 2010 DWH blowout. *PLoS ONE* **2015**, *10*, e0132341. [[CrossRef](#)]
13. Murawski, S.A.; Fleeger, J.W.; Patterson, W.F.; Hu, C.; Daly, K.L.; Romero, I.; Toro-Farmer, G. How did the Deepwater Horizon oil spill affect coastal and continental shelf ecosystems of the Gulf of Mexico? *Oceanography* **2015**, *29*, 160–173. [[CrossRef](#)]
14. Wade, T.L.; Sericano, J.L.; Sweet, S.T.; Knap, A.H.; Guinasso, N.L. Spatial and temporal distribution of water column total polycyclic aromatic hydrocarbons (PAH) and total petroleum hydrocarbons (TPH) from the Deepwater Horizon (Macondo) incident. *Mar. Pollut. Bull.* **2016**, *103*, 286–293. [[CrossRef](#)] [[PubMed](#)]
15. Romero, I.C.; Schwing, P.T.; Brooks, G.R.; Larson, R.A.; Hastings, D.W.; Ellis, G.; Goddard, E.; Hollander, D.J. Hydrocarbons in deep-sea sediments following the 2010 Deepwater Horizon Blowout in the Northeast Gulf of Mexico. *PLoS ONE* **2015**, *10*, e0128371. [[CrossRef](#)] [[PubMed](#)]
16. Romero, I.C.; Sutton, T.; Carr, B.; Quintana-Rizzo, E.; Ross, S.W.; Hollander, D.J.; Torres, J.J. Decadal assessment of polycyclic aromatic hydrocarbons in mesopelagic fishes from the Gulf of Mexico reveals exposure to oil-derived sources. *Environ. Sci. Technol.* **2018**, *52*, 10985–10996. [[CrossRef](#)] [[PubMed](#)]
17. Stout, S.A.; Payne, J.R. Macondo oil in deep-sea sediments: Part 1—Sub-sea weathering of oil deposited on the seafloor. *Mar. Pollut. Bull.* **2016**, *108*, 365–380. [[CrossRef](#)]
18. Stout, S.A.; Payne, J.R. Chemical composition of floating and sunken in-situ burn residues from the Deepwater Horizon oil spill. *Mar. Pollut. Bull.* **2016**, *111*, 186–202. [[CrossRef](#)]

19. Passow, U.; Ziervogel, K.; Asper, V.; Diercks, A. Marine snow formation in the aftermath of the Deepwater Horizon oil spill in the Gulf of Mexico. *Environ. Res. Lett.* **2012**, *7*, 3. [[CrossRef](#)]
20. Daly, K.L.; Passow, U.; Chanton, J.; Hollander, D. Assessing the impacts of oil-associated marine snow formation and sedimentation during and after the Deepwater Horizon Oil spill. *Anthropocene* **2016**, *13*, 18–33. [[CrossRef](#)]
21. Brakstad, O.G.; Lewis, A.; Beegle-Krause, C.J. A critical review of marine snow in the context of oil spills and oil spill dispersant treatment with focus on the Deepwater Horizon oil spill. *Mar. Pollut. Bull.* **2018**, *135*, 346–356. [[CrossRef](#)]
22. Passow, U.; Hetland, R.D. What happened to all of the oil? *Oceanography* **2016**, *29*, 88–95. [[CrossRef](#)]
23. White, H.K.; Hsing, P.-Y.; Cho, W.; Shank, T.M.; Cordes, E.E.; Quattrini, A.M.; Nelson, R.K.; Camilli, R.; Demopoulos, A.W.J.; German, C.R.; et al. Impact of the Deepwater horizon oil spill on a deep-water coral community in the Gulf of Mexico. *Proc. Natl. Acad. Sci. USA* **2012**, *109*, 20303–20308. [[CrossRef](#)] [[PubMed](#)]
24. Valentine, D.L.; Fisher, G.B.; Bagby, S.C.; Nelson, R.K.; Reddy, C.M.; Sylva, S.P.; Woo, M.A. Fallout plume of submerged oil from Deepwater Horizon. *Proc. Natl. Acad. Sci. USA* **2014**, *111*, 15906–15911. [[CrossRef](#)] [[PubMed](#)]
25. Chanton, J.; Zhao, T.; Rosenheim, B.E.; Joye, S.; Bosman, S.; Brunner, C. Using natural abundance radiocarbon to trace the flux of petrocarbon to the sea floor following the Deepwater Horizon oil spill. *Environ. Sci. Technol.* **2015**, *49*, 847–854. [[CrossRef](#)] [[PubMed](#)]
26. Romero, I.C.; Toro-Farmer, G.; Diercks, A.R.; Schwing, P.; Muller-Karger, F.; Murawski, S.; Hollander, D.J. Large-scale deposition of weathered oil in the Gulf of Mexico following a deep-water oil spill. *Environ. Pollut.* **2017**, *228*, 179–189. [[CrossRef](#)] [[PubMed](#)]
27. Xu, C.; Zhang, S.; Beaver, M.; Wozniak, A.S.; Obeid, W.; Lin, Y.; Wade, T.L.; Schwehr, K.A.; Lin, P.; Sun, L.; et al. Decreased sedimentation efficiency of petro- and non-petro-carbon caused by a dispersant for Macondo surrogate oil in a mesocosm simulating a coastal microbial community. *Mar. Chem.* **2018**, *206*, 34–43. [[CrossRef](#)]
28. Xu, C.; Zhang, S.; Beaver, M.; Lin, P.; Sun, L.; Doyle, S.M.; Sylvan, J.B.; Wozniak, A.S.; Hatcher, P.G.; Kaiser, K.; et al. The role of microbially-mediated exopolymeric substances (EPS) in regulating Macondo oil transport in a mesocosm experiment. *Mar. Chem.* **2018**, *206*, 52–61. [[CrossRef](#)]
29. Burd, A.B.; Chanton, J.P.; Daly, K.L.; Gilbert, S.; Passow, U.; Quigg, A. The science behind marine-oil snow and MOSFFA: Past, present, and future. *Prog. Oceanogr.* **2020**, *187*, 102398. [[CrossRef](#)]
30. Bacosa, H.P.; Erdner, D.L.; Liu, Z. Differentiating the roles of photooxidation and biodegradation in the weathering of Light Louisiana Sweet crude oil in surface water from the Deepwater Horizon site. *Mar. Pollut. Bull.* **2015**, *95*, 265–272. [[CrossRef](#)]
31. Bacosa, H.P.; Thyng, K.; Plunkett, S.; Erdner, D.L.; Liu, Z. The tarballs on Texas beaches following the 2014 Texas City “Y” Spill: Modeling, chemical, and microbiological studies. *Mar. Pollut. Bull.* **2016**, *109*, 236–244. [[CrossRef](#)]
32. Liu, J.; Bacosa, H.P.; Liu, Z. Potential environmental factors affecting oil-degrading bacterial populations in deep and surface waters of the northern Gulf of Mexico. *Front. Microbiol.* **2017**, *7*, 2131. [[CrossRef](#)]
33. Sun, L.; Chiu, M.; Xu, C.; Lin, P.; Schwehr, K.; Bacosa, H.; Kamalanathan, M.; Quigg, A.; Chin, W.-C.; Santschi, P.H. The effects of sunlight on the composition of exopolymeric substances and subsequent aggregate formation during oil spills. *Mar. Chem.* **2018**, *203*, 49–54. [[CrossRef](#)]
34. Quigg, A.; Passow, U.; Chin, W.-C.; Xu, C.; Doyle, S.; Bretherton, L.; Kamalanathan, M.; Williams, A.K.; Sylvan, J.B.; Finkel, Z.V.; et al. The role of microbial exopolymers in determining the fate of oil and chemical dispersants in the ocean. *Limnol. Oceanogr. Lett.* **2016**, *1*, 3–26. [[CrossRef](#)]
35. Bacosa, H.P.; Kamalanathan, M.; Chiu, M.H.; Tsai, S.M.; Sun, L.; Labonté, J.M.; Schwehr, K.A.; Hala, D.; Santschi, P.H.; Chin, W.C.; et al. Extracellular polymeric substances (EPS) producing and oil degrading bacteria isolated from the northern Gulf of Mexico. *PLoS ONE* **2018**, *13*, e0208406. [[CrossRef](#)] [[PubMed](#)]
36. Kamalanathan, M.; Chiu, M.-H.; Bacosa, H.; Schwehr, K.; Tsai, S.-M.; Doyle, S.; Yard, A.; Mapes, S.; Vasequez, C.; Bretherton, L.; et al. Role of polysaccharides in diatom *Thalassiosira pseudonana* and its associated bacteria in hydrocarbon presence. *Plant Physiol.* **2019**, *180*, 1898–1911. [[CrossRef](#)] [[PubMed](#)]
37. Xu, C.; Lin, P.; Zhang, S.; Sun, L.; Xing, W.; Schwehr, K.A.; Chin, W.-C.; Wade, T.L.; Knap, A.H.; Hatcher, P.G.; et al. The interplay of extracellular polymeric substances and oil/Corexit to affect the petroleum incorporation into sinking marine oil snow in four mesocosms. *Sci. Total Environ.* **2019**, *693*, 133626. [[CrossRef](#)] [[PubMed](#)]

38. Shiu, R.-F.; Chiu, M.-H.; Vazquez, C.I.; Tsai, Y.-Y.; Le, A.; Wa-Kagiri, A.; Xu, C.; Kamalanathan, M.; Bacosa, H.; Doyle, S.; et al. Protein to carbohydrate (P/C) ratio changes in microbial extracellular polymeric substances induced by oil and Corexit. *Mar. Chem.* **2020**, *223*, 103789. [[CrossRef](#)]
39. Schwehr, K.A.; Xu, C.; Chiu, M.-H.; Zhang, S.; Sun, L.; Lin, P.; Beaver, M.; Jackson, C.; Agueda, O.; Bergen, C.; et al. Protein: Polysaccharide ratio in exopolymeric substances controlling the surface tension of seawater in the presence or absence of surrogate Macondo oil with and without Corexit. *Mar. Chem.* **2018**, *206*, 84–92. [[CrossRef](#)]
40. Passow, U. Formation of rapidly-sinking, oil-associated marine snow. *Deep Sea Res. II* **2016**, *129*, 232–240. [[CrossRef](#)]
41. Ziervogel, K.; McKay, L.; Rhodes, B.; Osburn, C.L.; Dickson-Brown, J.; Arnosti, C.; Teske, A. Microbial activities and dissolved organic matter dynamics in oil-contaminated surface seawater from the Deepwater Horizon oil spill site. *PLoS ONE* **2012**, *7*, e34816. [[CrossRef](#)]
42. Fu, J.; Gong, Y.; Zhao, X.; O'Reilly, S.E.; Zhao, D. Effects of oil and dispersant on formation of marine oil snow and transport of oil hydrocarbons. *Environ. Sci. Technol.* **2014**, *48*, 14392–14399. [[CrossRef](#)]
43. Wirth, M.A.; Passow, U.; Jeschek, J.; Hand, I.; Schulz-Bull, D.E. Partitioning of oil compounds into marine oil snow: Insights into prevailing mechanisms and dispersant effects. *Mar. Chem.* **2018**, *206*, 62–73. [[CrossRef](#)]
44. Genzer, J.L.; Kamalanathan, M.; Bretherton, L.; Hillhouse, J.; Xu, C.; Santschi, P.H.; Quigg, A. Diatom aggregation when exposed to crude oil and chemical dispersant: Potential impacts of ocean acidification. *PLoS ONE* **2020**, *15*, e0235473. [[CrossRef](#)] [[PubMed](#)]
45. Passow, U.; Sweet, J.; Quigg, A. How the dispersant Corexit impacts the formation of sinking marine oil snow. *Mar. Pollut. Bull.* **2017**, *125*, 139–145. [[CrossRef](#)] [[PubMed](#)]
46. Wade, T.L.; Shi, D.; Gold-Bouchot, G.; Morales-McDevitt, M.E.; Sweet, S.T.; Bera, G.; Wang, B.; Quigg, A.; Knap, A.H. A method for the production of large volumes of WAF and CEWAF for dosing mesocosms to understand marine oil snow formation. *Heliyon* **2017**, *3*, e00419. [[CrossRef](#)]
47. Hatcher, P.G.; Obeid, W.; Wozniak, A.S.; Xu, C.; Zhang, S.; Santschi, P.H.; Quigg, A. Identifying oil/marine snow associations in mesocosm simulations of the Deepwater Horizon oil spill event using solid-state ¹³C NMR spectroscopy. *Mar. Pollut. Bull.* **2018**, *126*, 159–165. [[CrossRef](#)]
48. Doyle, S.M.; Whitaker, E.A.; de Pascuale, V.; Wade, T.L.; Knap, A.H.; Santschi, P.H.; Quigg, A.; Sylvan, J.B. Rapid formation of microbe-oil aggregates and changes in community composition in coastal surface water following exposure to oil and the dispersant corexit. *Front. Microbiol.* **2018**, *689*, 9. [[CrossRef](#)]
49. Kamalanathan, M.; Xu, C.; Schwehr, K.; Bretherton, L.; Beaver, M.; Doyle, S.M.; Genzer, J.; Hillhouse, J.; Sylvan, J.B.; Santschi, P.; et al. Extracellular enzyme activity profile in a chemically enhanced water accommodated fraction of surrogate oil: Toward understanding microbial activities after the Deepwater Horizon Oil Spill. *Front. Microbiol.* **2018**, *9*, 798. [[CrossRef](#)]
50. Bretherton, L.; Kamalanathan, M.; Genzer, J.; Hillhouse, J.; Setta, S.; Liang, Y.; Brown, C.M.; Xu, C.; Sweet, J.; Passow, U.; et al. Response of natural phytoplankton communities exposed to crude oil and chemical dispersants during a mesocosm experiment. *Aquat. Toxicol.* **2019**, *206*, 43–53. [[CrossRef](#)]
51. Wozniak, A.S.; Prem, P.M.; Obeid, W.; Quigg, A.; Xu, C.; Santschi, P.H.; Schwehr, K.A.; Hatcher, P.G. Rapid degradation of oil in mesocosm simulations of marine oil snow events. *Environ. Sci. Technol.* **2019**, *53*, 3441–3450. [[CrossRef](#)]
52. Wade, T.L.; Sweet, S.T.; Sericano, J.L.; Guinasso, N., Jr.; Diercks, A.-R.; Highsmith, R.C.; Asper, V.; Joung, D.; Shiller, A.M.; Lohrenz, S.E.; et al. Analyses of water samples from the Deepwater Horizon oil spill: Documentation of the subsurface plume. *Geophys. Monogr. Ser.* **2011**, *195*, 77–82.
53. Bacosa, H.P.; Erdner, D.L.; Rosenheim, B.E.; Shetty, P.; Seitz, K.W.; Baker, B.J.; Liu, Z. Hydrocarbon degradation and response of seafloor sediment bacterial community in the northern Gulf of Mexico to light Louisiana sweet crude oil. *ISME J.* **2018**, *12*, 2532–2543. [[CrossRef](#)] [[PubMed](#)]
54. Cullen, J.A.; Marshall, C.D.; Hala, D. Integration of multi-tissue PAH and PCB burdens with biomarker activity in three coastal shark species from the northwestern Gulf of Mexico. *Sci. Total Environ.* **2019**, *650*, 1158–1172. [[CrossRef](#)] [[PubMed](#)]
55. Wang, Z.D.; Fingas, M.; Lambert, P.; Zeng, G.; Yang, C.; Hollebhone, B. Characterization and identification of the Detroit River mystery oil spill (2002). *J. Chromatogr. A* **2004**, *1038*, 201–214. [[CrossRef](#)] [[PubMed](#)]
56. Hammer, Ø.; Harper, D.A.T.; Ryan, P.D. PAST: Paleontological statistics software package for education and data analysis. *Palaeontol. Electron.* **2001**, *4*, 1–9.

57. Zhang, Z.; Inole, C.; Li, G. Coordination of in phenanthrene biodegradation; pyruvate as microbial demarcation. *Bull. Environ. Contam. Toxicol.* **2010**, *85*, 581–584. [[CrossRef](#)] [[PubMed](#)]
58. Zhang, Z.; Zhao, X.; Liang, Y.; Li, G.; Zhou, J. Microbial functional genes reveal selection of microbial community by PAHs in polluted soils. *Environ. Chem. Lett.* **2013**, *11*, 11–17. [[CrossRef](#)]
59. Bacosa, H.P.; Suto, K.; Inoue, C. Degradation potential and microbial community structure of heavy-oil enriched microbial consortia from mangrove sediments in Okinawa, Japan. *J. Environ. Sci. Health A* **2013**, *48*, 835–846. [[CrossRef](#)]
60. Bacosa, H.P.; Inoue, C. Polycyclic aromatic hydrocarbons (PAHs) biodegradation potential and diversity of microbial consortia enriched from tsunami sediments in Miyagi, Japan. *J. Hazard. Mater.* **2015**, *283*, 689–697. [[CrossRef](#)]
61. Bacosa, H.P.; Inoue, C. Heavy oil degrading *Burkholderia* and *Pseudomonas* strains: Insights on the degradation potential of isolates and microbial consortia. *Palawan Sci.* **2020**, *12*, 74–89.
62. Ghosal, D.; Ghosh, S.; Dutta, T.K.; Ahn, Y. Current state of knowledge in microbial degradation of polycyclic aromatic hydrocarbons (PAHs): A review. *Front. Microbiol.* **2016**, *7*, 1369. [[CrossRef](#)]
63. Williams, A.K.; Bacosa, H.P.; Quigg, A. The impact of dissolved inorganic nitrogen and phosphorus on responses of microbial plankton to the Texas City “Y” oil spill in Galveston Bay, Texas (USA). *Mar. Pollut. Bull.* **2017**, *121*, 32–44. [[CrossRef](#)] [[PubMed](#)]
64. Steichen, J.L.; Labonté, J.M.; Windham, R.; Hala, D.; Kaiser, K.; Setta, S.; Faulkner, P.; Bacosa, H.; Yan, G.; Kamalanathan, M.; et al. Microbial, physical, and chemical changes in Galveston Bay following an extreme flooding event, Hurricane Harvey. *Front. Mar. Sci.* **2020**, *7*, 186. [[CrossRef](#)]
65. Bacosa, H.P.; Steichen, J.; Kamalanathan, M.; Windham, R.; Lubguban, A.; Labonté, J.M.; Kaiser, K.; Hala, D.; Santschi, P.H.; Quigg, A. Polycyclic aromatic hydrocarbons (PAHs) and putative PAH-degrading bacteria in Galveston Bay, TX (USA), following Hurricane Harvey (2017). *Environ. Sci. Pollut. Res.* **2020**, *27*, 34987–34999. [[CrossRef](#)] [[PubMed](#)]
66. Loh, A.; Yim, U.H.; Ha, S.Y.; An, J.G. A preliminary study on the role of suspended particulate matter in the bioavailability of oil-derived polycyclic aromatic hydrocarbons to oysters. *Sci. Total Environ.* **2018**, *643*, 1084–1090. [[CrossRef](#)] [[PubMed](#)]
67. Cai, Z.; Fu, J.; Liu, W.; Fu, K.; O’Reilly, S.E.; Zhao, D. Effects of oil dispersants on settling of marine sediment particles and particle-facilitated distribution and transport of oil components. *Mar. Pollut. Bull.* **2017**, *114*, 408–418. [[CrossRef](#)] [[PubMed](#)]
68. Adhikari, P.L.; Maiti, K.; Bosu, S.; Jones, P.R. 234Th as a tracer of vertical transport of polycyclic aromatic hydrocarbons in the northern Gulf of Mexico. *Mar. Pollut. Bull.* **2016**, *107*, 179–187. [[CrossRef](#)] [[PubMed](#)]
69. Yamada, M.; Takada, H.; Toyoda, K.; Yoshida, A.; Shibata, A.; Nomura, H.; Wada, M.; Nishimura, M.; Okamoto, K.; Ohwada, K. Study on the fate of petroleum-derived polycyclic aromatic hydrocarbons (PAHs) and the effect of chemical dispersant using an enclosed ecosystem, mesocosm. *Mar. Pollut. Bull.* **2003**, *47*, 105–113. [[CrossRef](#)]
70. Adhikari, P.L.; Maiti, K.; Overton, E.B.; Rosenheim, B.E.; Marx, B.D. Distributions and accumulation rates of polycyclic aromatic hydrocarbons in the northern Gulf of Mexico sediments. *Environ. Pollut.* **2016**, *212*, 413–423. [[CrossRef](#)]
71. Means, J.C.; Wood, S.G.; Hasset, J.J.; Banwart, W.L. Sorption of polynuclear aromatic hydrocarbons by sediments and soils. *Environ. Sci. Technol.* **1980**, *14*, 1524–1528. [[CrossRef](#)]
72. Loh, A.; Shankar, R.; Ha, S.Y.; An, J.G.; Yim, U.H. Stability of mechanically and chemically dispersed oil: Effect of particle types on oil dispersion. *Sci. Total Environ.* **2020**, *716*, 135343. [[CrossRef](#)]
73. Loh, A.; Yim, U.H. A review of the effects of particle types on oil-suspended particulate matter aggregate formation. *Ocean Sci. J.* **2016**, *51*, 535–548. [[CrossRef](#)]
74. Stoffyn-Egli, P.; Lee, K. Formation and characterization of oil-mineral aggregates. *Spill Sci. Technol. Bull.* **2002**, *8*, 31–44. [[CrossRef](#)]
75. Gustitus, S.A.; Clement, T.P. Formation, fate, and impacts of microscopic and macroscopic oil-sediment residues in nearshore marine environments: A critical review. *Rev. Geophys.* **2017**, *55*, 1130–1157. [[CrossRef](#)]
76. Passow, U.; Sweet, J.; Francis, S.; Xu, C.; Dissanayake, A.L.; Lin, Y.Y.; Santschi, P.H.; Quigg, A. Incorporation of oil into diatom aggregates. *Mar. Ecol. Prog. Ser.* **2019**, *612*, 65–86. [[CrossRef](#)]
77. National Research Council. *Oil Spill Dispersants; Efficacy and Effects*; The National Academy Press: Washington, DC, USA, 2005.

78. Zhao, X.; Gong, Y.Y.; O'Reilly, S.E.; Zhao, D.Y. Effects of oil dispersant on solubilization, sorption and desorption of polycyclic aromatic hydrocarbons in sediment–seawater systems. *Mar. Pollut. Bull.* **2015**, *92*, 160–169. [[CrossRef](#)] [[PubMed](#)]
79. Gong, Y.; Zhao, X.; Cai, Z.; O'Reilly, S.E.; Hao, X.; Zhao, D. A review of oil, dispersed oil and sediment interactions in the aquatic environment: Influence on the fate, transport and remediation of oil spills. *Mar. Pollut. Bull.* **2014**, *79*, 16–33. [[CrossRef](#)]
80. Arnosti, C.; Ziervogel, K.; Yang, T.; Teske, A. Oil-derived marine aggregates—Hotspots of polysaccharide degradation by specialized bacterial communities. *Deep Sea Res. Part II* **2016**, *129*, 179–186. [[CrossRef](#)]
81. Ziervogel, K.; Joye, S.B.; Kleindienst, S.; Malkin, S.Y.; Passow, U.; Steen, A.D.; Arnosti, C. Polysaccharide hydrolysis in the presence of oil and dispersants: Insights into potential degradation pathways of exopolymeric substances (EPS) from oil-degrading bacteria. *Elem. Sci. Anthropos.* **2019**, *7*, 31. [[CrossRef](#)]
82. Bacosa, H.P.; Liu, Z.; Erdner, D.L. Natural sunlight shapes crude oil-degrading bacterial communities in northern Gulf of Mexico surface waters. *Front. Microbiol.* **2015**, *6*, 1325. [[CrossRef](#)]
83. Santschi, P.H.; Xu, C.; Schwehr, K.A.; Lin, P.; Sun, L.; Chin, W.-C.; Kamalanathan, M.; Bacosa, H.P.; Quigg, A. Can the protein/carbohydrate (P/C) ratio of exopolymeric substances (EPS) be used as a proxy for their 'stickiness' and aggregation propensity? *Mar. Chem.* **2020**, *218*, 103734. [[CrossRef](#)]
84. Kleindienst, S.; Seidel, M.; Ziervogel, K.; Grim, S.; Loftis, K.; Harrison, S.; Malkin, S.Y.; Perkins, M.J.; Field, J.; Sogin, M.L.; et al. Chemical dispersants can suppress the activity of natural oil-degrading microorganisms. *Proc. Natl. Acad. Sci. USA* **2015**, *112*, 14900–14905. [[CrossRef](#)] [[PubMed](#)]
85. Overholt, W.A.; Marks, K.P.; Romero, I.C.; Hollander, D.J.; Snell, T.W.; Kostka, J.E. Hydrocarbon-degrading bacteria exhibit a species-specific response to dispersed oil while moderating ecotoxicity. *Appl. Environ. Microbiol.* **2016**, *82*, 518–527. [[CrossRef](#)] [[PubMed](#)]
86. Adhikari, P.L.; Maiti, K.; Overton, E.B. Vertical fluxes of polycyclic aromatic hydrocarbons in the northern Gulf of Mexico. *Mar. Chem.* **2015**, *168*, 60–68. [[CrossRef](#)]
87. Parinos, C.; Gogou, A.; Bouloubassi, I.; Stavrakakis, S.; Plakidi, E.; Hatzianestis, I. Sources and downward fluxes of polycyclic aromatic hydrocarbons in the open southwestern Black Sea. *Org. Geochem.* **2013**, *57*, 65–75. [[CrossRef](#)]
88. Bouloubassi, I.; Méjanelle, L.; Pete, R.; Fillaux, J.; Lorre, A.; Point, V. Point PAH transport by sinking particles in the open Mediterranean Sea: A 1 year sediment trap study. *Mar. Pollut. Bull.* **2006**, *52*, 560–571. [[CrossRef](#)]
89. Dachs, J.; Bayona, J.M.; Ittekkot, I.; Albaigés, J. Monsoon-driven vertical fluxes of organic pollutants in the western Arabian Sea. *Environ. Sci. Technol.* **1999**, *33*, 3949–3956. [[CrossRef](#)]
90. Raoux, C.; Bayona, J.M.; Miguel, J.C.; Teyssie, J.L.; Fowler, S.W.; Albaiges, J. Particulate fluxes of aliphatic and aromatic hydrocarbons in near-shore waters to the Northwestern Mediterranean Sea, and the effect of continental runoff. *Estuar. Coast. Shelf Sci.* **1999**, *48*, 605–616. [[CrossRef](#)]
91. Pettersen, H.; Neaff, C.; Broman, D. Impact of PAH outlets from an oil refinery on the receiving water area—sediment trap fluxes and multivariate statistical analysis. *Mar. Pollut. Bull.* **1997**, *34*, 85–95. [[CrossRef](#)]
92. Bacosa, H.; Suto, K.; Inoue, C. Preferential degradation of aromatic hydrocarbons in kerosene by a microbial consortium. *Int. Biodeterior. Biodegr.* **2010**, *64*, 702–710. [[CrossRef](#)]
93. Schwing, P.T.; Romero, I.C.; Brooks, G.R.; Hastings, D.W.; Larson, R.A.; Hollander, D.J. A decline in benthic foraminifera following the Deepwater Horizon event in the northeastern Gulf of Mexico. *PLoS ONE* **2015**, *10*, e0120565. [[CrossRef](#)]
94. Gemell, B.J.; Bacosa, H.P.; Liu, Z.; Buskey, E.J. Can gelatinous zooplankton influence the fate of crude oil in marine environments. *Mar. Pollut. Bull.* **2016**, *113*, 483–487. [[CrossRef](#)] [[PubMed](#)]
95. Seeley, M.E.; Wang, Q.; Bacosa, H.; Rosenheim, B.E.; Liu, Z. Environmental petroleum pollution analysis using ramped pyrolysis-gas chromatography-mass spectrometry. *Org. Chem.* **2018**, *124*, 180–189. [[CrossRef](#)]
96. Van Eenennaam, J.S.; Rohal, M.; Montagna, P.A.; Radović, J.R.; Oldenburg, T.B.; Romero, I.C.; Murk, A.J.; Foekema, E. Ecotoxicological benthic impacts of experimental oil-contaminated marine snow deposition. *Mar. Pollut. Bull.* **2019**, *141*, 164–175. [[CrossRef](#)] [[PubMed](#)]

